Communications In Catalysis
Vol. 3, No. 1, 2026, pp. 73-89
DOI: 10.22049/cic.2026.32267.1047
Azarbaijan Shahid Madani University

Structure-Performance Relationships in Covalent Triazine Frameworks: Synthesis, Applications, and Perspectives

Hasan Valizadeh[1], Nazila Taghavi Kalajahi[2*]

[1,2]Chemistry Department, Basic Science Faculty, Shahid Madani University, Tabriz, Iran

Email: nazila.taghavi@azaruniv.ac.ir

Received: 2026-05-29, Accepted: 2026-06-18

Abstract

Covalent triazine frameworks (CTFs) are nitrogen-rich porous organic polymers constructed from aromatic 1,3,5-triazine units linked by covalent bonds. Since CTF-1 was reported in 2008, their synthesis has advanced through ionothermal and superacid-promoted nitrile cyclotrimerization, P_2O_5-mediated amide conversion, amidine–aldehyde polycondensation, Friedel–Crafts functionalization of cyanuric chloride, and condensation of preformed triazine units. These routes produce materials with varying structural order, pore architectures, and surface areas. Their applications in gas adsorption and separation, heterogeneous catalysis, photocatalysis, and electrocatalysis depend not only on surface area but also on pore dimensions, framework composition, accessible active sites, electronic structure, and stacking. This review explores how monomer design and synthetic conditions determine CTF architecture and how structural and textural properties govern performance. It compares representative synthetic strategies, resulting material properties, and limitations in available evidence, while highlighting challenges to achieving reliable operation under practical conditions. Particular emphasis is placed on relationships between structural characteristics and application-specific requirements.

Keywords: Covalent triazine frameworks; porous organic polymers; porosity; heterogeneous catalysis; photocatalysis; structure–performance relationships

1. Introduction

Porous materials are commonly classified by pore width according to IUPAC recommendations as microporous (< 2 nm), mesoporous (2–50 nm), or macroporous (> 50 nm) [1]. These boundaries are conventional classifications rather than sharp physical transitions. Among the materials developed over recent decades, porous organic polymers (POPs), assembled from light elements such as carbon, hydrogen, oxygen, nitrogen, and boron through covalent bonds, have attracted interest because they can combine low density, thermal and chemical stability, and permanent porosity with substantial control over molecular structure [4–6]. The POP family includes covalent organic frameworks (COFs), first reported by Yaghi and co-workers in 2005 [2], as well as conjugated microporous polymers, porous aromatic frameworks, hyper-cross-linked polymers, and polymers of intrinsic microporosity [4].

Covalent triazine frameworks (CTFs), introduced by Kuhn, Antonietti, and Thomas in 2008 [3], are an important nitrogen-rich subclass of POPs. They contain aromatic 1,3,5-triazine units connected through organic linkers; in the original CTF-1 synthesis, the triazine rings formed by cyclotrimerization of aromatic nitriles in molten $ZnCl_2$ at approximately 400 °C. Compared with many imine- or boronate-linked COFs, CTFs are generally more resistant to hydrolysis because their networks contain chemically robust aromatic and triazine linkages. Many reported CTFs withstand exposure to water and a range of acidic or basic conditions, although stability depends on the precise structure and synthesis history [4–6]. Their triazine nitrogens can provide polar adsorption sites and contribute to Lewis-basic catalytic behaviour. The electron-deficient triazine unit can also influence the electronic structure of the framework, but semiconducting and photocatalytic properties depend on the conjugated linker, stacking, and degree of carbonization rather than on the triazine ring alone [4–6].

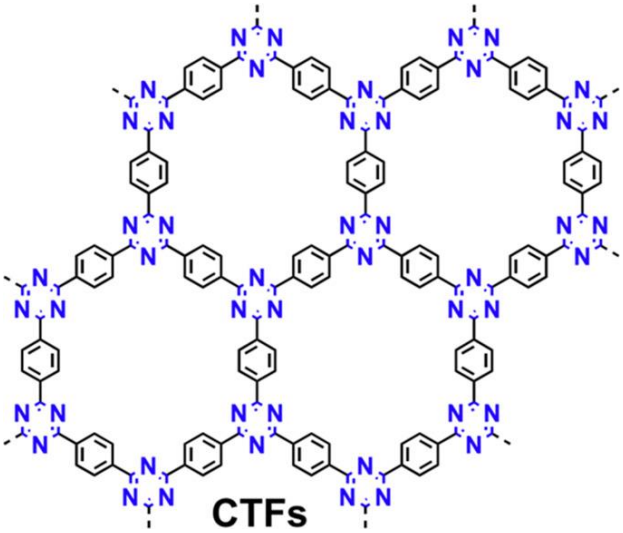

Figure 1. Schematic structure of a covalent triazine framework (CTF) composed of aromatic 1,3,5-triazine nodes connected by phenylene linkers. Reproduced from Liao et al. [6], Fig. 1, under the Creative Commons Attribution 4.0 International License (CC BY 4.0; https://creativecommons.org/licenses/by/4.0/).

Existing reviews have largely emphasized either CTF synthesis or particular application areas. Here, the discussion is organized around the relationship between molecular structure, pore architecture, and material performance. Section 2 considers how monomer design and reaction conditions influence porosity and framework properties. Section 3 compares the principal synthetic routes and the materials obtained by each method. Section 4 discusses representative applications, focusing on the structural features that appear to influence performance. The final section identifies unresolved limitations and research priorities.

2. Structural factors governing porosity and performance

The relationship between framework structure, porosity, and performance is closely coupled, but it is not governed by a single variable. Monomer length, rigidity, symmetry, and functionality can affect the geometry of the developing network; reaction temperature, time, concentration, and catalyst or solvent conditions determine how that network forms and reorganizes. These factors together influence the surface area, pore-size distribution, and relative proportions of micro- and mesopores. In a systematic ionothermal study of aromatic nitriles, temperature and monomer concentration had a stronger influence on porosity than monomer size or geometry within the series examined [12]. This finding should not be generalized to every CTF synthesis, where monomer structure may play a larger role.

Pore dimensions affect both adsorption thermodynamics and the rate at which molecules reach internal surfaces. Ultramicropores, particularly those below about 0.5 nm, can strengthen low-pressure CO_2 adsorption when their dimensions are well matched to the adsorbate. Larger micropores and mesopores can improve diffusion and provide access for bulkier molecules or reaction intermediates. Mesoporosity is therefore useful in many catalytic systems, but it is not a universal requirement: the optimum pore network depends on the size of the target molecule and on whether equilibrium capacity or transport rate is the principal objective.

The chemical environment of the framework also matters. Nitrogen content and the distribution of nitrogen functionalities affect polarity and the basicity of potential active sites, while linker conjugation and layer stacking influence electronic properties. Crystallinity may improve charge transport in some photocatalytic systems, but greater structural order does not automatically produce higher activity: it can coincide with lower accessible surface area or changes in pore accessibility. These effects need to be assessed for each application rather than treated as universal design rules.

The perfluorinated framework FCTF-1 shows how pore dimensions and surface chemistry are able to act together in gas capture. It combines polar C–F bonds with a substantial fraction of ultramicropores below 0.5 nm and has been reported to adsorb 1.76 mmol g^{-1} of CO_2 at 273 K and 0.1 bar. Its CO_2/N_2 selectivity was 77 in mixed-gas breakthrough experiments under kinetic-flow conditions; by comparison, the selectivity predicted from single-gas equilibrium adsorption data was 31 [7]. These distinct values describe different measurement approaches and should not be conflated. A separate comparison of crystalline and amorphous CTF-0 samples prepared from the same monomer reported surface areas of approximately 500 and 2000 $m^2\ g^{-1}$, respectively, together with differences in CO_2 uptake and cycloaddition catalysis [8]. Because the samples also differ in structural order and pore architecture, this comparison does not isolate surface area as the sole cause of the performance differences. It nevertheless shows that changes in porosity and framework organization can substantially affect function even when the nominal chemical composition is retained.

Crystallinity adds another variable, particularly in applications that involve charge transport. Greater order can improve the pathways available for charge migration, but the conditions used to promote crystallinity may reduce surface area or change the number of accessible sites. A two-step treatment converted staggered AB-stacked CTF-1 into an eclipsed AA-stacked material with high crystallinity and a reported surface area of 646 $m^2\ g^{-1}$ [10]. The original CTF-HUST materials

provide a contrasting example: they were described as layered, but the authors reported that they did not exhibit long-range crystalline order by PXRD; broad diffraction features were considered consistent with the possibility of partial layer organization [11]. A later, distinct monomer-feeding strategy produced highly crystalline CTF-HUST-HC1 [18]. These studies show that stacking and structural order can be influenced by synthesis, although their benefits must be considered alongside changes in porosity and composition.

3. Synthetic routes toward covalent triazine frameworks

CTF synthesis can be grouped according to how the triazine unit is introduced. In one class of methods, the triazine ring forms during framework synthesis, most commonly through cyclotrimerization of nitrile precursors or, in a reported alternative, through P_2O_5-catalyzed direct condensation of aromatic amides [4,6,17]. In another class, a preformed triazine unit is present in the starting material and is connected to organic linkers through reactions such as Friedel–Crafts substitution [4,6]. Amidine–aldehyde polycondensation is a related route in which triazine rings form during condensation. This classification is useful for comparing reaction design, although some nitrogen-rich triazine polymers made by condensation are more appropriately regarded as related materials than as CTFs in the strict structural sense.

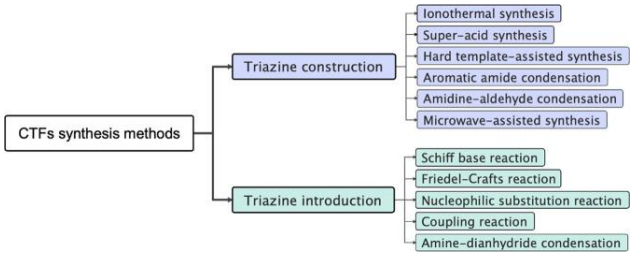

Figure 2. Classification of CTF synthesis strategies according to whether the triazine unit is constructed during polymerization or introduced through a preformed triazine-containing monomer. Reproduced from Liao et al. [6], Fig. 3, under the Creative Commons Attribution 4.0 International License (CC BY 4.0; https://creativecommons.org/licenses/by/4.0/).

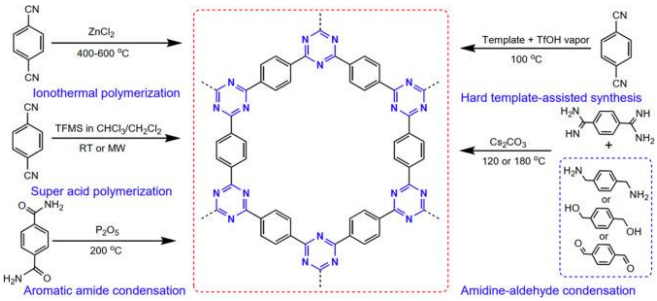

Figure 3. Representative routes for constructing triazine units during CTF synthesis: ionothermal and superacid-catalyzed nitrile cyclotrimerization, hard-template-assisted synthesis, aromatic amide condensation, and amidine–aldehyde condensation. Reproduced from Liao et al. [6], Fig. 4, under the Creative Commons Attribution 4.0 International License (CC BY 4.0; https://creativecommons.org/licenses/by/4.0/).

3.1. Ionothermal synthesis

The original and still widely used route is the ionothermal cyclotrimerization of aromatic nitriles in molten $ZnCl_2$ [3]. In a sealed glass ampoule, the nitrile monomer is heated with molten $ZnCl_2$, which serves as both the reaction medium and a Lewis-acid promoter of triazine-ring formation. CTF-1 prepared from 1,4-dicyanobenzene at about 400 °C was reported to have a BET surface area of 791 m^2 g^{-1} and a pore volume of 0.40 cm^3 g^{-1} under the reported monomer-to-$ZnCl_2$ ratio [3]. The same study reported an H_2 uptake of 1.55 wt% at 77 K and 1 bar for a network prepared from 4,4′-dicyanobiphenyl (DCBP), not for CTF-1; these results therefore refer to different framework compositions [3]. At higher temperatures, further structural reorganization and carbonization can occur, producing materials with larger pore volumes and surface

areas; values as high as about 3300 $m^2\ g^{-1}$ and 2.4 $cm^3\ g^{-1}$, respectively, were reported for mesoporous products [13]. A systematic investigation of reaction conditions further showed that processing parameters strongly influence the final porosity [12]. The precise balance between triazine formation and subsequent carbonization is therefore central to controlling the product.

The ionothermal approach has been extended to a range of aromatic nitriles. CTF-2, prepared from 2,6-naphthalenedicarbonitrile, forms layered structures; the crystalline product was reported to have a relatively low surface area of about 90 $m^2\ g^{-1}$, whereas high-temperature treatment produced an amorphous material with a surface area of up to 2255 $m^2\ g^{-1}$ [14]. CTF-0, obtained from 1,3,5-tricyanobenzene, has a high density of triazine units and a reported nitrogen content of 19.3 wt%. Depending on the monomer-to-$ZnCl_2$ ratio and reaction temperature, crystalline samples with surface areas near 500 $m^2\ g^{-1}$ or amorphous samples approaching 2000 $m^2\ g^{-1}$ have been reported; the materials also differ in CO_2 uptake and catalytic behaviour [8]. These values describe products obtained under different structural and thermal conditions and should not be read as a direct comparison of surface area alone. The main practical limitations of ionothermal synthesis are the high reaction temperature, the need for thermally robust monomers, removal of residual $ZnCl_2$, and the difficulty of scaling sealed-ampoule procedures. These constraints have encouraged the development of milder routes.

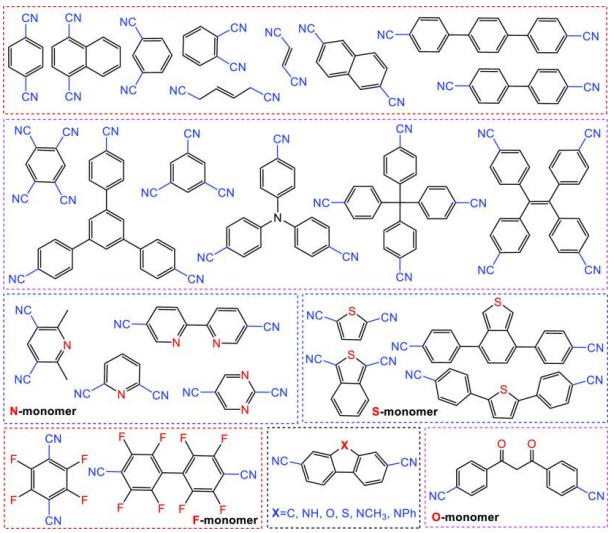

Figure 4. Representative aromatic nitrile monomers used in ionothermal polymerization, including hydrocarbon-based and heteroatom-containing building blocks. Reproduced from Liao et al. [6], Fig. 5, under the Creative Commons Attribution 4.0 International License (CC BY 4.0; https://creativecommons.org/licenses/by/4.0/).

3.2. Superacid-catalyzed synthesis

In 2012, Cooper and co-workers reported that strong Brønsted acids, particularly trifluoromethanesulfonic acid (TfOH), promote the cyclotrimerization of aromatic nitriles at room temperature or under microwave-assisted conditions [15]. The resulting materials were amorphous, microporous, and fluorescent, with BET surface areas exceeding 1100 $m^2\ g^{-1}$ and CO_2 uptakes of up to 4.17 mmol g^{-1} at 273 K and 1 bar. Because the reaction takes place well below the temperatures used for ionothermal synthesis, it can preserve functional groups that would otherwise be vulnerable to thermal degradation. The method also avoids a molten metal salt, simplifying product washing. Dai and co-workers adapted superacid-promoted triazine formation to prepare porous framework membranes; these materials showed an ideal CO_2/N_2 selectivity of 29 ± 2 and a CO_2 permeability of 518 ± 25 barrer [16]. A limitation of the superacid route is that the

products are generally amorphous, and acid-sensitive monomers are unsuitable. A later two-step strategy partially addressed the structural-order limitation: treatment with a catalytic amount of TfOH at 250 °C produced a staggered AB-stacked CTF-1, which was then annealed at 350 °C under nitrogen to obtain a more crystalline AA-stacked material with a surface area of 646 $m^2 g^{-1}$ [10]. This approach improves structural order.

3.3. P_2O_5-mediated synthesis from aromatic amides

Phosphorus pentoxide is a strong dehydrating reagent, but the study by Yu and co-workers described the transformation as a P_2O_5-catalyzed direct condensation of aromatic amides, rather than establishing an isolated nitrile intermediate. Terephthalamide was used to construct the crystalline framework pCTF-1, with a BET surface area of 2034.1 $m^2 g^{-1}$ [17]. The reported material adsorbed 21.9 wt% CO_2 at 273 K and 1.75 wt% H_2 at 77 K under the low-pressure conditions described by the authors [17]. Model reactions showed that both benzamide and benzonitrile could be converted to 1,3,5-triphenyl-2,4,6-triazine under the P_2O_5-catalyzed conditions. The method therefore provides an alternative entry to triazine frameworks from aromatic amide precursors without requiring prior isolation of the corresponding nitrile monomer.

3.4. Amidine-aldehyde polycondensation

A different strategy, reported in 2017, uses polycondensation between aromatic aldehydes and amidine or amidinium building blocks. In the original CTF-HUST synthesis, the reactants were combined in DMSO with Cs_2CO_3 as base at approximately 120 °C under ambient pressure [11]. The products were reported to have layered structures and surface areas in the range of 663–807 $m^2 g^{-1}$, and the synthesis was demonstrated at gram scale. Importantly, PXRD showed that these first-generation CTF-HUST materials did not possess long-range crystalline order; the authors described broad features as only suggestive of partially layered structures [11]. The materials were evaluated as photocatalysts for sacrificial hydrogen evolution, with a maximum reported rate of 2647 $\mu mol\ h^{-1}\ g^{-1}$ under visible light, and a pyrolyzed derivative was tested as an anode material for sodium-ion batteries [11]. In a later, separate study, direct control of the monomer-feeding rate in an open system produced the highly crystalline CTF-HUST-HC1 with abundant exposed {001} facets; the improved charge separation and transfer were associated with enhanced photocatalytic removal of nitric oxide relative to less crystalline analogues [18]. Because structural order, facet exposure, and charge-carrier behaviour changed together, the individual contribution of crystallinity cannot be isolated from the activity data alone.

3.5. Friedel-Crafts alkylation with cyanuric chloride

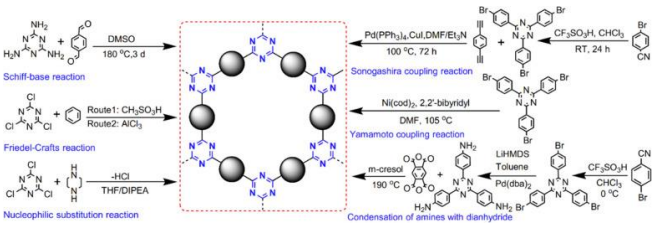

Figure 5. Representative routes using preformed triazine-containing monomers, including Schiff-base condensation, Friedel–Crafts reaction, nucleophilic substitution, cross-coupling, and amine–dianhydride condensation. Reproduced from Liao et al. [6], Fig. 10, under the Creative Commons Attribution 4.0 International License (CC BY 4.0; https://creativecommons.org/licenses/by/4.0/).

A second group of strategies uses a preformed triazine unit. Cyanuric chloride (2,4,6-trichloro-1,3,5-triazine) provides an electron-

deficient node whose three C–Cl bonds can react with electron-rich aromatic linkers under Friedel–Crafts conditions. Anhydrous $AlCl_3$ and methanesulfonic acid have both been used to promote this type of network formation. The approach is operationally straightforward and can produce amorphous, porous materials; surface area and pore-size distribution depend on monomer concentration and linker structure [4]. Mechanochemical processing has also been applied to this chemistry: ball milling of carbazole with cyanuric chloride was reported to produce porous triazine-based polymers in nearly quantitative yield without bulk solvent [19]. More recently, a molecular-confinement strategy enabled the preparation of highly crystalline, carboxyl-functionalized CTFs in about 30 minutes and at kilogram scale. In that system, carboxyl groups on the aromatic monomer were proposed to influence electrophilic substitution and to provide anchoring effects that direct ordered framework growth [20]. These advances broaden the scope of Friedel–Crafts-based CTF synthesis, although the monomer design and reaction conditions required for crystallinity may limit how generally the method can be applied. A related triazine- and carbazole-functionalized porous polymer was reported to adsorb 18.0 wt% CO_2 at 273 K and 1 bar and to show CO_2/N_2 adsorption selectivity [21].

3.6. Schiff-base and related condensation routes

Triazine-rich porous networks can also be prepared from melamine, which already contains a 1,3,5-triazine core bearing three amino groups. Condensation of melamine with di- or trivalent aromatic aldehydes has been used to produce highly cross-linked microporous networks. One reported family of melamine-based materials had surface areas up to 1377 $m^2\ g^{-1}$, micropore volumes up to 0.41 $cm^3\ g^{-1}$, and nitrogen contents as high as 40 wt% [22]. Related diaminotriazine-based aminal-linked porous polymers (APOPs) have reported surface areas of 724–1402 $m^2\ g^{-1}$ and isosteric heats of CO_2 adsorption up to 33.3 kJ mol^{-1} [23]. These results illustrate how nitrogen-rich nodes and polar linker groups can increase interactions with CO_2. The classification of these materials requires care: they contain triazine units and nitrogen-rich pores, but their aminal or imine linkages differ from the triazine-forming backbones of conventional ionothermal CTFs. They are therefore best discussed as closely related triazine-rich porous polymers rather than automatically grouped with all CTFs.

The routes differ in the structures they can access and in the practical demands they impose. Ionothermal synthesis remains useful when thermally robust monomers and chemically stable frameworks are priorities, but its temperature and salt-removal requirements are significant constraints. Superacid-promoted and condensation-based methods broaden the range of functional monomers that can be used, although the resulting materials may have limited long-range order or require careful control of reaction conditions. P_2O_5-mediated synthesis offers an amide-based route to triazine frameworks [17]. The original amidine–aldehyde polycondensation produced layered materials without long-range crystalline order, whereas a later monomer-feeding protocol achieved highly crystalline CTF-HUST-HC1 [11,18]. Friedel–Crafts approaches are attractive because recent work has addressed both solvent use and structural order [19,20]. the appropriate route depends on the required pore structure, functionality, crystallinity, stability, and scale of production.

4. Structure-porosity-performance relationships in applications

4.1. Adsorption and gas separation

CO_2 capture is one of the most extensively studied adsorption applications of CTFs. Across the literature, higher surface area and micropore volume often accompany higher uptake at moderate pressure, whereas low-pressure affinity and selectivity are also influenced by pore size and surface chemistry. Superacid-derived frameworks have been reported to adsorb up to 4.17 mmol g^{-1} of CO_2 at 273 K and 1 bar [15]. In an adamantane-cored PCTF series, PCTF-5 showed the largest BET surface area (1183 m^2 g^{-1}) and CO_2 uptake (58.1 cm^3 g^{-1} at 273 K and 1 bar). PCTF-7, by contrast, had a lower surface area (613 m^2 g^{-1}) and uptake (48.9 cm^3 g^{-1}), but gave the highest ideal CO_2/N_2 selectivity (41:1; compared with 32:1 for PCTF-5) in the zero-pressure limit ($P \rightarrow 0$) [24]. These ideal selectivities were calculated by IAST from single-component adsorption isotherms and were not measured in mixed-gas breakthrough experiments [24]. FCTF-1 provides a different design example: its ultramicropores and fluorinated surface were associated with a kinetic CO_2/N_2 selectivity of 77 in mixed-gas breakthrough tests, whereas the value predicted from single-gas equilibrium data was 31 [7]. Charged CTFs based on viologen derivatives reached CO_2 uptakes of 133 mg g^{-1} at 273 K and 1 bar, with reported surface areas up to 1247 m^2 g^{-1} [25]. In this series, summarized in Table 1, raising the ionothermal synthesis temperature from 400 to 500 °C increased the BET surface area (744 → 1247 m^2 g^{-1}) and total pore volume (0.36 → 1.04 cm^3 g^{-1}) and shifted the framework from predominantly microporous to hierarchically micro/mesoporous [25]. CO_2 uptake did not follow surface area, however: the microporous cCTF-400 adsorbed 126 mg g^{-1} at 273 K, nearly the same as cCTF-500 (133 mg g^{-1}), and also had the highest isosteric heat of adsorption at zero coverage (49 kJ mol^{-1}, compared with 43 kJ mol^{-1} for cCTF-500) [25]. The intermediate sample cCTF-450 showed the lowest uptake (99 mg g^{-1}) despite a larger surface area than cCTF-400. The authors attributed the high CO_2 affinity to electrostatic interactions between CO_2 and the charged viologen sites, whereas the decrease in Q_st across the series was associated with nitrogen loss and the development of mesoporosity [25].

For context, triptycene-derived benzimidazole-linked polymers, which are POPs but not CTFs, were reported to reach 5.12 mmol g^{-1} under the stated comparison conditions [26]. Triazine-framework membranes offer a distinct separation format, with a reported CO_2 permeability of 518 barrer and an ideal CO_2/N_2 selectivity of 29 [16]. These results should not be ranked as if they were measured in a single experiment: activation procedures, pressure ranges, gas mixtures, and definitions of selectivity differ among studies. Taken together, however, they suggest that pore volume contributes to capacity, while ultramicropore dimensions and polar or ionic sites can be especially important for low-pressure adsorption and selectivity. Mesopores may improve mass transport, although their effect on equilibrium capacity depends on the material and measurement conditions.

4.2. Heterogeneous (thermo)catalysis

A widely studied catalytic transformation with CTFs is the cycloaddition of CO_2 to epoxides to form cyclic carbonates. Triazine nitrogens can contribute Lewis-basic sites, while pore dimensions and connectivity influence the accessibility of epoxide and CO_2 molecules to

those sites. Roeser, Kailasam, and Thomas reported higher activity for CTF catalysts with larger surface areas and additional mesoporosity; they also found that a more basic pyridine-containing framework was more active at lower temperature than a phenylene-based analogue [9]. These results indicate that both substrate accessibility and the chemical environment of the framework influence catalytic performance. Ionic functionalization provides another way to modify this environment. Viologen-based charged CTFs combine cationic sites with hierarchical porosity and were reported to catalyze the conversion of CO_2 and epoxides into cyclic carbonates in high yields with exclusive product selectivity [25]. Imidazolium-based cationic CTFs, prepared from an imidazolium-functionalized dinitrile, also catalyzed the cycloaddition without an external additive under mild conditions [27]. Carbazole-decorated CTFs (CTF-CSUs) achieved yields up to 99% at 0.1 MPa and 25 °C and retained catalytic activity over five reuse cycles; the same materials were also evaluated for oxygen reduction [28]. These examples show that ionic or heteroaromatic functionalities can complement the triazine-containing framework, although catalytic results should be compared only with due attention to reaction conditions and substrate scope.

CTFs have also been used as porous supports for metal nanoparticles and molecular metal complexes. In these systems, the catalytically active centres may be the supported metal species rather than the triazine nitrogens themselves. Metal dispersion, the local coordination environment, pore accessibility, and resistance to aggregation or leaching can therefore influence the observed activity and recyclability. Isolated Ir sites anchored on a CTF have, for example, been examined using experimental and computational methods [29]. A broader range of metal-containing CTF catalysts and triazine-based porous polymers for organic transformations is reviewed in Refs. [30,31]. Table 2 summarizes the 23 catalytic systems compiled in Table 1 of Tahir et al. [31], including oxidation, hydrogenation, isomerization, hydroformylation, dehydrogenation, carbonylation, C–H borylation, and Mannich-type reactions. The reported activities were measured under different conditions and are not intended as a direct ranking of catalyst performance.

Table 2. Summary of various catalytic reactions performed by utilizing CTFs.

Adapted from Table 1 of Tahir et al. [31]. The individual reference column in the original table has been omitted; material labels and monomer structures are retained as reported.

Material	Monomer	Metal content	Type of reaction	Activity
Pd/CTF	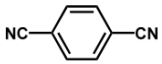	1 wt% Pd (nanoparticles)	Oxidation of glycerol into glyceric acid	Rate of glycerol consumption: 982 $mol \cdot h^{-1} \cdot mol^{-1}$ Selectivity = 81%
Pd/CTF	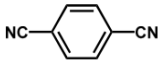	1 wt% Pd (nanoparticles)	Oxidation of benzyl alcohol	TOF = 1453 h^{-1} Selectivity = 98%
Pd/CTF	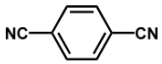	4 wt% Pd (nanoparticles)	Hydrogenation of N-heterocycles (1,10-phenanthroline)	Pressure/selectivity: 30 bar/98.9%; 20 bar/97.9% (for 8H-phen) TOF = 47.6 h^{-1} (1st cycle)
Pd/CTF	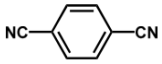	2.05 wt% Pd (nanoparticles)	Selective double carbonylation of aryl iodides	Several substrates tested Yield up to 90%; selectivity = 95%
Ru/CTF-c	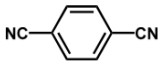	3.91 wt% Ru (nanoparticles)	Oxidation of 5-hydroxymethylfurfural to 2,5-furandicarboxylic acid	Conversion > 99% Yield = 41.4%
Ru/CTF-c	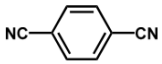	5 wt% Ru (coordination using $(RuCl_2(p\text{-cymene}))_2$)	Hydrogenolysis of xylitol	Full conversion 15% selectivity to propylene glycol
CTF-DCE-Ag	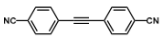	4.3 wt% Ag (nanoparticles)	Carboxylation of terminal alkynes	TON = 247 Yield > 98.9
Pt-CTF	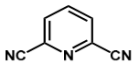	–	Low-temperature oxidation of methane to methanol	Selectivity > 75% TON = 246
Ir@CTF	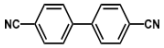	2.4 wt% Ir	Isomerization of 1-octen-3-ol to 3-octanone	TOF = 24 min^{-1}

Material	Monomer	Metal content	Type of reaction	Activity
Rh@CTF-c		3.5 wt% Rh	Hydroformylation of crude 1-octene	Conversion = 62% TOF = 600 h^{-1} TON = 12,000
CTF-Ir	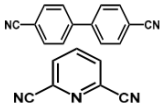	16 wt% Ir	Dehydrogenation of formic acid	TOF = 27,000 h^{-1} TON = 1,060,000
Ir@meso-CTF	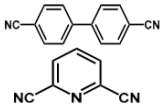	2 wt% Ir	Hydrogenation of CO_2	TON = 358
Ir@meso-CTF@monolith	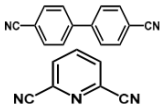	0.23 μmol / 0.045 mg Ir	Dehydrogenation of formic acid	TOF = 207,200 h^{-1} TON = 2,230
Bpy-CTF-(IrCp*Cl)Cl	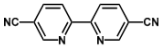	4.7 wt% Ir	Hydrogenation of CO_2 to formate	TOF = 5,300 h^{-1} TON = 5,000
(bpy-CTF-Ru(acac)$_2$)Cl	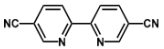	1.68 wt% Ru	Hydrogenation of CO_2 to formate	TOF = 22,700 h^{-1} TON = 21,200
(bpy-CTF-RuCl$_3$)	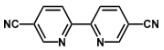	2.1 wt% Ru	Hydrogenation of CO_2 to formate	TOF = 38,800 h^{-1} TON = 20,000
(bpy-CTF(RhCp*Cl)Cl) & (bpy-CTF(IrCp*Cl)Cl)	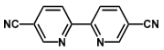	1.78 wt% Rh & 4.7 wt% Ir	Transfer hydrogenation of carbonyl compounds	Conversion = 99% Rh catalyst is more active than Ir catalyst; only the Ir catalyst maintained activity during recycling
(bpy-CTF-Al(OTf)$_2$)(Co(CO)$_4$)	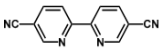	3.76 wt% Al & 2.67 wt% Co	Carbonylation of epoxides into β-lactones	Conversion > 99% Selectivity = 90%

Material	Monomer	Metal content	Type of reaction	Activity
Ir(I)@bipyCTF	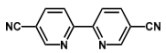	8.26 wt% Ir	C–H borylation of 1,2-dichlorobenzene	TON = 64 Yield = 95%
$Ir_{0.68}$-NHC-CTF	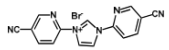	0.68 wt% Ir	Hydrogenation of CO_2 to formate	TOF = 1,600 h^{-1} TON = 24,300
Rh-bpim-CTF	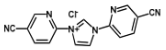	0.61 wt% Rh	Carbonylation of methanol	Conversion = 93% TOF = 2,100 h^{-1}
(imidazolium-CTF)($Co(CO)_4$)	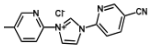	3.62 wt% Co	Direct synthesis of methyl 3-hydroxybutyrate from propylene oxide	Conversion > 99% Selectivity = 86%
V@acacCTF	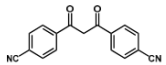	1.6 wt% V	Mannich reaction between 2-naphthol and N-methylmorpholine N-oxide	TON = 213 Conversion = 100% Yield = 95%

Note: Material annotations follow the nomenclature used in the source literature.

Abbreviations: TOF, turnover frequency; TON, turnover number; HMF, 5-hydroxymethylfurfural; FDCA, 2,5-furandicarboxylic acid.

4.3. Photocatalysis

The electron-deficient triazine unit can contribute to the electronic structure of CTFs, making many members of this family candidates for visible-light photocatalysis. Their optical and catalytic properties, however, vary with linker conjugation, functional-group substitution, stacking, and structural order; not every CTF should be assumed to behave as an equivalent n-type semiconductor. An early example of a molecular transformation was the visible-light-driven, metal-free oxidation of alcohols to aldehydes and ketones using molecular oxygen over a thiophene-containing CTF [32]. Subsequent work has examined the effects of morphology, band structure, and charge separation on photocatalytic activity [33,39]. Introducing thiophene or benzothiadiazole units into CTF backbones has been used to promote directional charge migration and improve photocatalytic hydrogen production [34]. Phosphorus doping has also been reported to increase H_2-evolution efficiency by 4.5-fold relative to undoped CTFs; the same study reported factors of 3.9 and 1.8 relative to phosphorus-doped g-C_3N_4 prepared from melamine and urea, respectively [35]. The CTF-HUST-HC1 results provide another example in which controlled monomer feeding, structural order, and charge-carrier behaviour are linked to photocatalytic performance [18]. A recent review discusses CTF-based solar photocatalysis [36], while another focuses on CTF-based composites [37]. Across these examples, improved activity is generally associated with some combination of light absorption, charge separation and transport, and accessibility of catalytic sites. The relative importance of each factor depends on the reaction and on the specific framework.

4.4. Electrocatalysis

Nitrogen-doped carbons obtained by pyrolysis of CTFs, as well as some intact CTFs, have been investigated as metal-free electrocatalysts. In a BINOL-derived CTF series with systematically varied nitrogen functionalities—including pyridinic or triazine nitrogen, pyrrolic nitrogen, quaternary nitrogen, and pyridine-N-oxide—the oxygen-reduction and hydrogen-evolution activities were associated with both nitrogen speciation and accessible porosity. The best material in that study reached a half-wave potential of 0.737 V for the four-electron ORR pathway and an HER overpotential of 0.31 V at 10 mA cm^{-2}, with a Tafel slope of 41 mV dec^{-1} [38]. Carbazole-containing CTFs have also shown ORR activity and methanol tolerance relative to a commercial Pt/C reference [28]. These examples indicate that intrinsic nitrogen-site chemistry and the accessibility of those sites both matter. Because pyrolysis can alter the original framework and generate new nitrogen environments, results for CTF-derived carbons should not be treated as direct evidence for the electrocatalytic behaviour of the unpyrolyzed CTF.

5. Conclusions and perspectives

CTFs have developed from the original high-temperature ionothermal materials into a broader family accessible through several distinct synthetic strategies. The examples reviewed here show that no single structural feature determines performance. High surface area can improve the number of accessible adsorption or catalytic sites, but pore dimensions and surface chemistry are also important. Greater crystallinity may benefit charge transport, yet can coincide with lower porosity or fewer accessible sites. Similarly, functional groups that strengthen interactions with CO_2 may occupy pore volume or change diffusion. Recent advances in controlled monomer feeding and molecularly confined

Friedel–Crafts synthesis demonstrate that these trade-offs can be managed more deliberately [18,20], although they have not been eliminated.

Several priorities will determine whether CTFs move beyond laboratory demonstrations. Synthetic methods that combine milder conditions, reproducible structural control, and scalable isolation remain important; mechanochemical processing and low-temperature polycondensation are promising starting points [11,19]. Equally important is a more quantitative treatment of structure–property relationships. Comparisons across the field are often complicated by differences in activation, pressure, temperature, gas composition, catalyst loading, and reactor design. More consistent reporting and the use of matched control materials would help distinguish the effects of surface area, pore-size distribution, crystallinity, and active-site chemistry. Finally, application studies need to test materials under realistic conditions, including humid gas streams, long photocatalytic runs, continuous-flow reactions, and extended electrocatalytic operation. CTFs are often chemically robust, but stability under a particular operating environment must be demonstrated for each framework and application [5,7]. For catalysis, rational design requires the monomer, reaction conditions, pore architecture, and active-site environment to be considered together; post-synthetic modification is one tool among several, not a substitute for controlling the initial framework structure.

References

[1] Thommes, M.; Kaneko, K.; Neimark, A. V.; Olivier, J. P.; Rodriguez-Reinoso, F.; Rouquerol, J.; Sing, K. S. W. Physisorption of Gases, with Special Reference to the Evaluation of Surface Area and Pore Size Distribution (IUPAC Technical Report). Pure Appl. Chem. 2015, 87 (9–10), 1051–1069. DOI: 10.1515/pac-2014-1117

[2] Côté, A. P.; Benin, A. I.; Ockwig, N. W.; O'Keeffe, M.; Matzger, A. J.; Yaghi, O. M. Porous, Crystalline, Covalent Organic Frameworks. Science 2005, 310, 1166–1170. DOI: 10.1126/science.1120411

[3] Kuhn, P.; Antonietti, M.; Thomas, A. Porous, Covalent Triazine-Based Frameworks Prepared by Ionothermal Synthesis. Angew. Chem. Int. Ed. 2008, 47 (18), 3450–3453. DOI: 10.1002/anie.200705710

[4] Liu, M.; Guo, L.; Jin, S.; Tan, B. Covalent Triazine Frameworks: Synthesis and Applications. J. Mater. Chem. A 2019, 7, 5153–5172. DOI: 10.1039/C8TA12442F

[5] Krishnaraj, C.; Jena, H. S.; Leus, K.; Van Der Voort, P. Covalent Triazine Frameworks: A Sustainable Perspective. Green Chem. 2020, 22, 1038–1071. DOI: 10.1039/C9GC03482J

[6] Liao, L.; Li, M.; Yin, Y.; Chen, J.; Zhong, Q.; Du, R.; Liu, S.; He, Y.; Fu, W.; Zeng, F. Advances in the Synthesis of Covalent Triazine Frameworks. ACS Omega 2023, 8 (5), 4527–4542. DOI: 10.1021/acsomega.2c06961

[7] Zhao, Y.; Yao, K. X.; Teng, B.; Zhang, T.; Han, Y. A Perfluorinated Covalent Triazine-Based Framework for Highly Selective and Water-Tolerant CO_2 Capture. Energy Environ. Sci. 2013, 6, 3684–3692. DOI: 10.1039/C3EE42548G

[8] Katekomol, P.; Roeser, J.; Bojdys, M. J.; Weber, J.; Thomas, A. Covalent Triazine Frameworks Prepared from 1,3,5-Tricyanobenzene. Chem. Mater. 2013, 25, 1542–1548. DOI: 10.1021/cm303751n

[9] Roeser, J.; Kailasam, K.; Thomas, A. Covalent Triazine Frameworks as Heterogeneous Catalysts for the Synthesis of Cyclic and Linear Carbonates from Carbon Dioxide and Epoxides. ChemSusChem 2012, 5, 1793–1799. DOI: 10.1002/cssc.201200091

[10] Yang, Z.; Chen, H.; Wang, S.; Guo, W.; Wang, T.; Suo, X.; Jiang, D.; Zhu, X.; Popovs, I.; Dai, S. Transformation Strategy for Highly Crystalline Covalent Triazine Frameworks: From Staggered AB to Eclipsed AA Stacking. J. Am. Chem. Soc. 2020, 142 (15), 6856–6860. DOI: 10.1021/jacs.0c00365

[11] Wang, K.; Yang, L.-M.; Wang, X.; Guo, L.; Cheng, G.; Zhang, C.; Jin, S.; Tan, B.; Cooper, A. I. Covalent Triazine Frameworks via a Low-Temperature Polycondensation Approach. Angew. Chem. Int. Ed. 2017, 56 (45), 14149–14153. DOI: 10.1002/anie.201708548

[12] Kuhn, P.; Thomas, A.; Antonietti, M. Toward Tailorable Porous Organic Polymer Networks: A High-Temperature Dynamic Polymerization Scheme Based on Aromatic Nitriles. Macromolecules 2009, 42 (1), 319–326. DOI: 10.1021/ma802322j

[13] Kuhn, P.; Forget, A.; Su, D.; Thomas, A.; Antonietti, M. From Microporous Regular Frameworks to Mesoporous Materials with Ultrahigh Surface Area: Dynamic Reorganization of Porous Polymer Networks. J. Am. Chem. Soc. 2008, 130, 13333–13337. DOI: 10.1021/ja803708s

[14] Bojdys, M. J.; Jeromenok, J.; Thomas, A.; Antonietti, M. Rational Extension of the Family of Layered, Covalent, Triazine-Based Frameworks with Regular Porosity. Adv. Mater. 2010, 22, 2202–2205. DOI: 10.1002/adma.200903436

[15] Ren, S.; Bojdys, M. J.; Dawson, R.; Laybourn, A.; Khimyak, Y. Z.; Adams, D. J.; Cooper, A. I. Porous, Fluorescent, Covalent Triazine-Based Frameworks via Room-Temperature and Microwave-Assisted Synthesis. Adv. Mater. 2012, 24 (17), 2357–2361. DOI: 10.1002/adma.201200751

[16] Zhu, X.; Tian, C.; Mahurin, S. M.; Chai, S.-H.; Wang, C.; Brown, S.; Veith, G. M.; Luo, H.; Liu, H.; Dai, S. A Superacid-Catalyzed Synthesis of Porous Membranes Based on Triazine Frameworks for CO_2 Separation. J. Am. Chem. Soc. 2012, 134 (25), 10478–10484. DOI: 10.1021/ja304879c

[17] Yu, S.-Y.; Mahmood, J.; Noh, H.-J.; Seo, J.-M.; Jung, S.-M.; Shin, S.-H.; Im, Y.-K.; Jeon, I.-Y.; Baek, J.-B. Direct Synthesis of a Covalent Triazine-Based Framework from Aromatic Amides. Angew. Chem. Int. Ed. 2018, 57, 8438–8442. DOI: 10.1002/anie.201801128

[18] Liu, M.; Jiang, K.; Ding, X.; Wang, S.; Zhang, C.; Liu, J.; Zhan, Z.; Cheng, G.; Li, B.; Chen, H.; Jin, S.; Tan, B. Controlling Monomer Feeding Rate to Achieve Highly Crystalline Covalent Triazine Frameworks. Adv. Mater. 2019, 31, 1807865. DOI: 10.1002/adma.201807865

[19] Troschke, E.; Grätz, S.; Lübken, T.; Borchardt, L. Mechanochemical Friedel–Crafts Alkylation—A Sustainable Pathway Towards Porous Organic Polymers. Angew. Chem. Int. Ed. 2017, 56 (24), 6859–6863. DOI: 10.1002/anie.201702303

[20] Zhang, L.; Sun, T.; Zhang, Z.; Zhang, Z.; Xu, Y. Rapid and Scalable Preparation of High-Crystalline Carboxyl-Functionalized Covalent Triazine Frameworks via Friedel–Crafts Reaction. Angew. Chem. Int. Ed. 2025, 64 (10), e202421251. DOI: 10.1002/anie.202421251

[21] Zhu, X.; Mahurin, S. M.; An, S.; Do-Thanh, C.-L.; Tian, C.; Li, Y.; Gill, L. W.; Hagaman, E. W.; Bian, Z.; Zhou, J.; Hu, J.; Liu, H.; Dai, S. Efficient CO_2 Capture by a Task-Specific Porous Organic Polymer Bifunctionalized with Carbazole and Triazine Groups. Chem. Commun. 2014, 50 (59), 7933–7936. DOI: 10.1039/C4CC01588F

[22] Schwab, M. G.; Fassbender, B.; Spiess, H. W.; Thomas, A.; Feng, X.; Müllen, K. Catalyst-Free Preparation of Melamine-Based Microporous Polymer Networks through Schiff Base Chemistry. J. Am. Chem. Soc. 2009, 131, 7216–7217. DOI: 10.1021/ja902116f

[23] Song, W.-C.; Xu, X.-K.; Chen, Q.; Zhuang, Z.-Z.; Bu, X.-H. Nitrogen-Rich Diaminotriazine-Based Porous Organic Polymers for Small Gas Storage and Selective Uptake. Polym. Chem. 2013, 4, 4690–4696. DOI: 10.1039/C3PY00590A

[24] Bhunia, A.; Boldog, I.; Möller, A.; Janiak, C. Highly Stable Nanoporous Covalent Triazine-Based Frameworks with an Adamantane Core for Carbon Dioxide Sorption and Separation. J. Mater. Chem. A 2013, 1, 14990–14999. DOI: 10.1039/C3TA13407E

[25] Büyükçakır, O.; Je, S. H.; Talapaneni, S. N.; Kim, D.-O.; Coşkun, A. Charged Covalent Triazine Frameworks for CO_2 Capture and Conversion. ACS Appl. Mater. Interfaces 2017, 9 (8), 7209–7216. DOI: 10.1021/acsami.6b16769

[26] Rabbani, M. G.; Reich, T. E.; Kassab, R. M.; Jackson, K. T.; El-Kaderi, H. M. High CO_2 Uptake and Selectivity by Triptycene-Derived Benzimidazole-Linked Polymers. Chem. Commun. 2012, 48, 1141–1143. DOI: 10.1039/C2CC16986J

[27] Liu, T.; Xu, R.; Yi, J.-D.; Liang, J.; Wang, X.; Shi, P.-C.; Huang, Y.-B.; Cao, R. Imidazolium-Based Cationic Covalent Triazine Frameworks for Highly Efficient Cycloaddition of Carbon Dioxide. ChemCatChem 2018, 10, 2036–2040. DOI: 10.1002/cctc.201800023

[28] Yu, W.; Gu, S.; Fu, Y.; Xiong, S.; Pan, C.; Liu, Y.; Yu, G. Carbazole-Decorated Covalent Triazine Frameworks: Novel Nonmetal Catalysts for Carbon Dioxide Fixation and Oxygen Reduction Reaction. J. Catal. 2018, 362, 1–9. DOI: 10.1016/j.jcat.2018.03.021

[29] Sackers, N. M.; Iemhoff, A.; Sautet, P.; Palkovits, R. Understanding the Structure of Isolated Iridium Sites Anchored on a Covalent Triazine Framework. Catal. Sci. Technol. 2023, 13, 2652–2655. DOI: 10.1039/D3CY00232B

[30] Puthiaraj, P.; Lee, Y.-R.; Zhang, S.; Ahn, W.-S. Triazine-Based Covalent Organic Polymers: Design, Synthesis and Applications in Heterogeneous Catalysis. J. Mater. Chem. A 2016, 4, 16288–16311. DOI: 10.1039/C6TA06089G

[31] Tahir, N.; Krishnaraj, C.; Leus, K.; Van Der Voort, P. Development of Covalent Triazine Frameworks as Heterogeneous Catalytic Supports. Polymers 2019, 11, 1326. DOI: 10.3390/polym11081326

[32] Huang, W.; Ma, B. C.; Lu, H.; Li, R.; Wang, L.; Landfester, K.; Zhang, K. A. I. Visible-Light-Promoted Selective Oxidation of Alcohols Using a Covalent Triazine Framework. ACS Catal. 2017, 7, 5438–5442. DOI: 10.1021/acscatal.7b01719

[33] Qian, Z.; Wang, Z.; Zhang, K. A. I. Covalent Triazine Frameworks as Emerging Heterogeneous Photocatalysts. Chem. Mater. 2021, 33, 1909–1926. DOI: 10.1021/acs.chemmater.0c04348

[34] Lan, Z.-A.; Xu, C.; Wu, M.; Zhang, X.; Chen, X.; Zhang, G.; Wang, X. Molecular Design of Covalent Triazine Frameworks with Anisotropic Charge Migration for Photocatalytic Hydrogen Production. Small 2022, 18, 2200129. DOI: 10.1002/smll.202200129

[35] Cheng, Z.; Fang, W.; Zhao, T.; Fang, S.; Bi, J.; Liang, S.; Li, L.; Yu, Y.; Wu, L. Efficient Visible-Light-Driven Photocatalytic Hydrogen Evolution on Phosphorus-Doped Covalent Triazine-Based Frameworks. ACS Appl. Mater. Interfaces 2018, 10, 41415–41421. DOI: 10.1021/acsami.8b16013

[36] Li, X.; Luo, X.; Liang, H.; Tan, R.; Zhou, F.; Zhang, Q.; Zhang, G.; Zhou, S.; Gu, P. Recent Advances in Covalent Triazine Frameworks for Solar-Driven Photocatalysis: Intrinsic Advantages, Modification Strategies, and Photocatalytic Applications. Solar RRL 2026, 10 (20), e70522. DOI: 10.1002/solr.70522

[37] Wei, Y.; Zhou, Q.; Wang, X.; Liao, Y.; Meng, J.; Huang, Y.; Gao, L.; Dai, W.-L. The Construction and Photocatalytic Application of Covalent Triazine Framework (CTF)-Based Composites: A Brief Review. Catalysts 2025, 15, 562. DOI: 10.3390/catal15060562

[38] Jena, H. S.; Krishnaraj, C.; Parwaiz, S.; Lecoeuvre, F.; Schmidt, J.; Pradhan, D.; Van Der Voort, P. Illustrating the Role of Quaternary-N of BINOL Covalent Triazine-Based Frameworks in Oxygen Reduction and Hydrogen Evolution Reactions. ACS Appl. Mater. Interfaces 2020, 12, 44689–44699. DOI: 10.1021/acsami.0c11381

[39] Liu, Y.; Wu, H.; Wang, Q. Strategies to Improve the Photocatalytic Performance of Covalent Triazine Frameworks. J. Mater. Chem. A 2023, 11, 21470–21497. DOI: 10.1039/D3TA04472F